OsteoArthritis and Cartilage (2004) **12,** 97–105

doi:10.1016/j.joca.2003.10.001

Osteoarthritis and Cartilage

International Cartilage Repair Society

OARSI OSTEOARTHRITIS RESEARCH SOCIETY INTERNATIONAL

X-ray detection of structural orientation in human articular cartilage

Carol Muehleman†,‡*, Sharmila Majumdar§, Ahi Sema Issever§, Fulvia Arfelli¶, Ralf-Hendrik Menk††, Luigi Rigon¶, Gabriele Heitner¶, Bernd Reime§§, Joachim Metge§§, Andreas Wagner‡‡, Klaus E. Kuettner‡ and Juergen Mollenhauer‡,‡‡

† *Department of Anatomy and Cell Biology, Rush Medical College, Chicago, IL 60612, USA*
‡ *Department of Biochemistry, Rush Medical College, Chicago, IL 60612, USA*
§ *Department of Radiology, Magnetic Resonance Science Center, University of California, San Francisco, CA 94143, USA*
¶ *Department of Physics, University of Trieste, Trieste, Italy*
†† *Sincrotrone Trieste SCpA, Trieste, Italy*
‡‡ *Department of Orthopaedics of the University of Jena at the Waldkrankenhaus 'Rudolf Elle', Jena, Germany*
§§ *Hamburger Synchrotronstrahlumgslabor HASYLAB at Deutsches Elektronen-Synchrotron DESY, Germany*

Summary

Objective: To determine the feasibility of detecting the structural orientation in cartilage with Diffraction Enhanced X-Ray Imaging.

Design: Human tali and femoral head specimens were Diffraction Enhanced X-Ray Imaged (DEI) at the SYRMEP beamline at Elettra at various energy levels to detect the architectural arrangement of collagen within cartilage. DEI utilizes a monochromatic and highly collimated beam, with an analyzer crystal that selectively weights out photons according to the angle they have been deviated with respect to the original direction. This provides images of very high contrast, and with the rejection of X-ray scatter.

Results: DEI allowed the visualization of articular cartilage and a structural orientation, resembling arcades, within.

Conclusion: Our diffraction enhanced images represent the first radiographic detection of the structural orientation in cartilage. Our data are in line with previous studies on the structural organization of joint cartilage. They confirm the model of a vaulting system of collagen fiber bundles interrupted by proteoglycan aggregates.

Key words: Collagen arcades, Cartilage, Diffraction enhanced imaging, Cartilage radiography.

Introduction

Articular cartilage provides a smooth, gliding surface for the articulating skeletal components of synovial joints. In addition, shock absorbance is provided through its characteristic compressibility upon load-bearing and re-swelling upon relaxation. Its zones from top down: superficial, transitional, deep and calcified, contain a sparse population of cells, the chondrocytes, within a matrix of proteoglycans and collagen fibers[1]. The overwhelming predominance of collagen fibers is collagen type II, and it is the intimate relationship between these fibers and the proteoglycans, aggrecan in particular, that provide the basis of cartilage structure and resiliency[2]. Since the time of Benninghoff[3] it has been accepted that there exists a three-dimensional collagen fiber structure whereby the fiber bundles form arcades, resembling gothic columns, in a vertical direction through the cartilage. It is this, to a wide extent intuitive, image that imparts the idea that the collagen framework can provide a very strong vaulting system to the cartilage.

Proteoglycans, due to their anionic charge, attract water into the cartilage matrix, thus creating a high osmotic pressure limited only by the framework of collagen fibers. During compression, the proteoglycans release water to the synovial fluid, and upon relaxation they pull water in. This model of osmotic pressure and collagen fibers, thus, renders the cartilage resistant to major irreversible deformation during load-bearing, and allows cartilage resiliency upon removal of load.

Demonstrating the arcade structure of collagen fibers in articular cartilage as been difficult. Polarizing light microscopy, monitoring birefingency, is capable of presenting the anisotropic pattern of the collagen fiber network[4]. However, it allows only very thin sections of cartilage to be studied which lack the overall three-dimensional framework of the collagen fibers. The suggestion of collagen arcades has also been viewed with scanning electron microscopy (SEM)[5–12] but it renders the viewing of even smaller regions of interest and is subject to preparation artifacts caused by the dehydration needed to prepare specimens.

Small angle X-ray diffraction also renders spatially-resolved information concerning the angular disposition of

*Address correspondence to: Dr C. Muehleman, Rush Medical College, Department of Anatomy, Suite 507 AF, 600 South Paulina, Chicago, IL 60612, USA. Tel.: +1-312-280-2958; Fax: +1-312-942-2040; E-mail: cmuehleman@rushu.rush.edu
Received 21 May 2003; revision accepted 26 September 2003.

collagen fibers in cartilage matrix whereby the depth of individual zones can be determined based on the averaged orientation of fibers within 2 μm increments[13].

More recently, high-resolution Magnetic Resonance Imaging (MRI) based on imaging the collagen fiber – bound highly coordinated water molecules has produced images of cartilage with a trilaminar appearance in the horizontal plane and a striated appearance in the vertical plane of the deep lamina[14,15]. It is the vertical plane striations that suggest a cartilage matrix organization corresponding to that observed microscopically. Several studies have shown a correlation of histologic zones with MR signal intensity in human and animal cartilage[16–20]. Modl *et al.*[21] showed that normal-looking knee and ankle articular cartilage from fresh cadavers showed three zones with 1.5 T and 0.156 mm pixel resolution MRI: a low-intensity zone near the articular surface that corresponded to the tangentially oriented collagen of the superficial histologic zone and a region of higher signal intensity deep to the superficial zone that correlated with the transitional zone. The deep radial, calcified cartilage and cortical bone were represented by a deep low-intensity zone on MRI.

Subsequent studies have shown that the number of laminae observed is inconsistent and dependent upon the location from which the sample was taken. In addition, the borders between the cartilage and fluid, and between the cartilage and subchondral bone may also be visible[22].

It is now known that this laminar appearance of cartilage on MRI is related to the T2 relaxation anisotropic arrangement of the collagen fibers and the water-proteoglycan interaction that amplifies this arrangement, along with the alignment of the specimen relative to the magnetic field[14,17,21–25]. Although it has also been demonstrated that truncation artifacts are capable of resulting in a laminar appearance of cartilage on MRI[26,27], a true laminar appearance originating from the architecture of the cartilage itself, and not from truncation artifacts, does indeed exist[27–31].

As cartilage is invisible with conventional radiography, detection of detail of this nature was not an option. However, we previously introduced the X-ray imaging of articular cartilage through a novel technology called Diffraction Enhanced X-ray Imaging (DEI)[32–34]. DEI renders radiographic images with dramatic gains in contrast over conventional radiography by utilizing X-ray refraction and scatter rejection, in addition to the absorption of conventional radiography. Currently, DEI utilizes a synchrotron X-ray beam that is made nearly monochromatic and highly collimated by two matching crystals. Here, we demonstrate, for the first time, the X-ray detection of a vertical structural orientation in human hip and ankle articular cartilage corresponding to that observed with MRI and microscopy.

Methods

SPECIMENS

The human specimens used in this study include a grossly normal[35] talus (obtained within 24 h of death of the donor through the Gift of Hope Organ and Tissue Donor Network of Illinois with institutional IRB approval) and six femoral heads from subjects who had undergone hip replacement surgery (five from the University of California, San Francisco and one from hip replacement surgery at the Waldkrankenhaus 'Rudolf Elle'. These femoral heads were chosen because each of them displayed at least some regions of morphologically normal cartilage among the degenerated regions. Pieces of morphologically normal-looking cartilage (as assessed through both gross visual[35] and histological inspection[36] with subchondral bone were removed from the formalin-preserved specimens by one of two methods. From the talus and one of the femoral heads, approximately 4 cm high by 6 cm wide by 1 cm thick cartilage/bone pieces were removed from the whole specimen with a small saw. Subsequently the bone was transected through the midline with the saw so that the cut ran through its length to reach a region approximating the border between the bone and calcified cartilage. The two sides of the bone were then pulled apart by hand (fracture method) so that the separation continued through the cartilage and rendered two separate pieces of cartilage/bone. This procedure was carried out so that the cartilage would separate along natural structural elements rather than being cut across such features. From each of the remaining five femoral heads, a core of cartilage/bone was removed by using a water-cooled drill saw (drill saw method), each core having a diameter of 15 mm and 14 mm in length. During imaging, the specimens were placed in thin plastic containers with polyethylene liners that both held the specimens in position and prevented dehydration. Each specimen was positioned so that the X-ray beam entered the specimen perpendicular to the height of the articular surface, in other words, in the same direction as the reader views the image.

EXPERIMENTAL SET-UP AND DEI METHOD

Diffraction enhanced images of the specimens have been obtained at the 6.1 bending magnet beamline 'SYRMEP' at Elettra, the third generation synchrotron light source operating in Trieste (Italy).

Two X-ray optical elements are required to perform DEI. The first is a monochromator, which prepares the monochromatic and highly collimated beam that traverses the sample. The second is an analyzer, which operates on the beam outgoing from the sample before it reaches the detector, selectively weighting the photons according to the angle they have been deviated with respect to the original direction. Typically, both the monochromator and the analyzer are perfect crystals.

In the present work, the monochromator consisted of a double Si [111] flat crystal, and the analyzer was a single crystal of the same confirmation. The system was operated in the non-dispersive Bragg geometry. Due to the laminar geometry of the beam, plane images were obtained by scanning both the object and the detector. The detector utilized was a 4 Megapixel CCD camera (Photonics Science, Ltd) with a 14×14 μm^2 pixel aperture coupled with a 20 m thick intensifier phosphor screen. The monochromator, sample, analyzer and detector were located at 16, 22, 22.5 and 23 m away from source, respectively.

As the double crystal monochromator is reached by the highly collimated, 'white' synchrotron radiation emitted at the bending magnet source, it provides a monochromatic beam with tunable energy. The latter is determined by the angle between the white beam and the lattice planes in the crystal (Bragg angle).

In this experiment the energies utilized were 17 keV and 25 keV. Once the energy is set, a curve for the transmitted

intensity (rocking curve) will be obtained by rocking the analyzer crystal around the Bragg angle[37].

The effectiveness of DEI lies in the fact that the width of the rocking curve is in the order of 1–00 μrad. In fact, when the sample is introduced in the beam, photons are deviated by an angle proportional to the gradient of the real part of the refraction index in the object plane, Typically, for biological tissue such refraction angles are in the order of microradians or tens of microradians, and thus comparable with the rocking curve width.

As demonstrated elsewhere[37] the narrow rocking curve of the analyzer crystal allows the recording of these tiny angular deviations by the photons in the sample as intensity modulations on the detector. They are absolutely imperceptible in conventional X-ray imaging and can thus be exploited to provide additional contrast besides the conventional x-ray absorption. Moreover photons deviated at a given refraction angle will contribute in a different way to images acquired with the analyzer set at different positions of the rocking curve. Particularly interesting are the images acquired at the peak and at half slope of the rocking curve. The image acquired at the peak features not only the conventional absorption contrast but also an additional 'extinction' contrast, which is due to the rejection of small angle scattering. The images acquired on the slopes highlight the contrast due to refraction. Finally, combining the two slope images according to simple equations[18] results in two new images called 'apparent absorption' image and 'refraction' image. The former displays the extinction contrast, while the latter is entirely due to refraction, and may be used to measure quantitatively the refraction angles at each point in the object plane.

HISTOLOGY

After DEI, the specimens were prepared for histology by decalcifying in aqueous formic acid/sodium citrate (50:50) or in 'Osteodec' for at least 48 h. The specimens were subsequently dehydrated in changes of ethanol at increasing concentration, paraffin embedded, sectioned to 5 μm thickness and stained with picrosirius red for polarizing microscopy or Safranin-O/fast green[38]. Specimens were then assessed for morphological degeneration.

Results

A Safranin O/fast green-stained section of articular cartilage and subchondral bone from the normal talus (Collins[35] gross visual grade=0, histological grade[36]=0) can be seen in Fig. 1A. The proteoglycans of the transitional and deep zones of cartilage are stained red with Safranin O, while the superficial zone, with little or no proteoglycan content, has an absence of Safranin O stain. Fig. 1B is a picrosirius red-stained section viewed under polarized light microscopy to display the typical birefringent pattern of collagen fibers in the superficial and deep zones. Fig. 1C is a DEI absorption image of the entire 5 mm thick specimen from which the section in 1B was taken. It shows the cartilage with an orientation, or faint vertical striations, throughout. The path of the X-ray beam was 90° to the image as viewed on the page. The bright line at the cartilage/subchondral bone interface is an X-ray refractile line. As expected, the DEI method is capable of allowing visualization of discontinuities in the sample, such as internal structures, invisible to conventional X-ray radiography, where strong X-ray scattering occurs. Since edges, in particular, are emphasized, the transition between cartilage and bone is emphasized in the images. In this image the gray scale was adjusted in order to allow good visibility of the cartilage while the bone appears black. This specimen was prepared by the 'fracture method' as described in the Methods section. In making a comparison between the polarizing light micrograph and the arcade structure in the DE image, it appears that the collagen fibers begin to arc at approximately 40% into the depth of the cartilage from the articular surface. This is in line with the approximate depth of the bottom of the transitional zone as detected with polarized light.

Fig. 2 is a collage consisting of an actual photograph (A), a Safranin O/fast green-stained section (B) and a DEI slope of the rocking curve image at 25 keV(C) of a femoral head from the. Although the cartilage surface was grossly normal[35] prior to and during imaging, the subchondral bone exhibited some abnormal features such as a cyst. The damage seen in the superficial region on the right side of the photograph and on the Safranin-O stained section was a result of processing the tissue after it had been imaged. The articular cartilage and its vertical striations are very apparent in the DEI refraction image due to the X-ray refraction at the edges of the fiber bundles. The conservation of cartilage and bone features throughout these three pictures is apparent.

Fig. 3A is an DEI apparent absorption image of the specimen in Fig. 2, showing the cartilage with vertical striations. Fig. 3B is a DEI refraction image. Here, the vertical striations are more apparent due to the X-ray refraction at the edges of the fiber bundles. 3C is an enlarged view of the image to show greater detail. It should be noted that these image have a different interpretation than an image based on absorption since the different gray levels represent variations of the X-ray deviations that occur within the sample. Thus, the contrast is not associated with the difference in the attenuation coefficient but in variations of refraction properties. As a consequence, all the borders are strongly enhanced in the cartilage as well as in the trabecular bone where a typical granularity is visible.

Fig. 4A is a Safranin-O stained section of a 'drill saw' prepared grossly and histologically normal femoral head specimen while 4B is a representative polarized light micrograph showing the birifringent pattern within the uncalcified cartilage. Fig. 4C and D are the DEI apparent absorption and refraction images, respectively, of the femoral head sample taken at 17 keV. Again, there is a visible orientation (arrows), but the region of arcing near the superficial zone is even more apparent here. This lower energy level renders excellent imaging of soft tissue. Due to the absence of X-ray scatter, even the apparent absorption image allows clear visualization of the arcade pattern. It is noteworthy that, within the refraction image, the structure of the subchondral bone, trabecular bone, and cartilage are simultaneously visible.

As the images represent information throughout the depth of the specimen (in the axis parallel to the path of the X-ray beam), all of the images may not necessarily be truly perpendicular views to the horizontal axis. Also, because it is difficult to place the vertical axis of the specimens precisely perpendicular to the beam, the superficial region appears wider, or of varying contrast, in some specimens as compared to others. In each image, however, vertical, or nearly vertical, striations are visible within the cartilage,

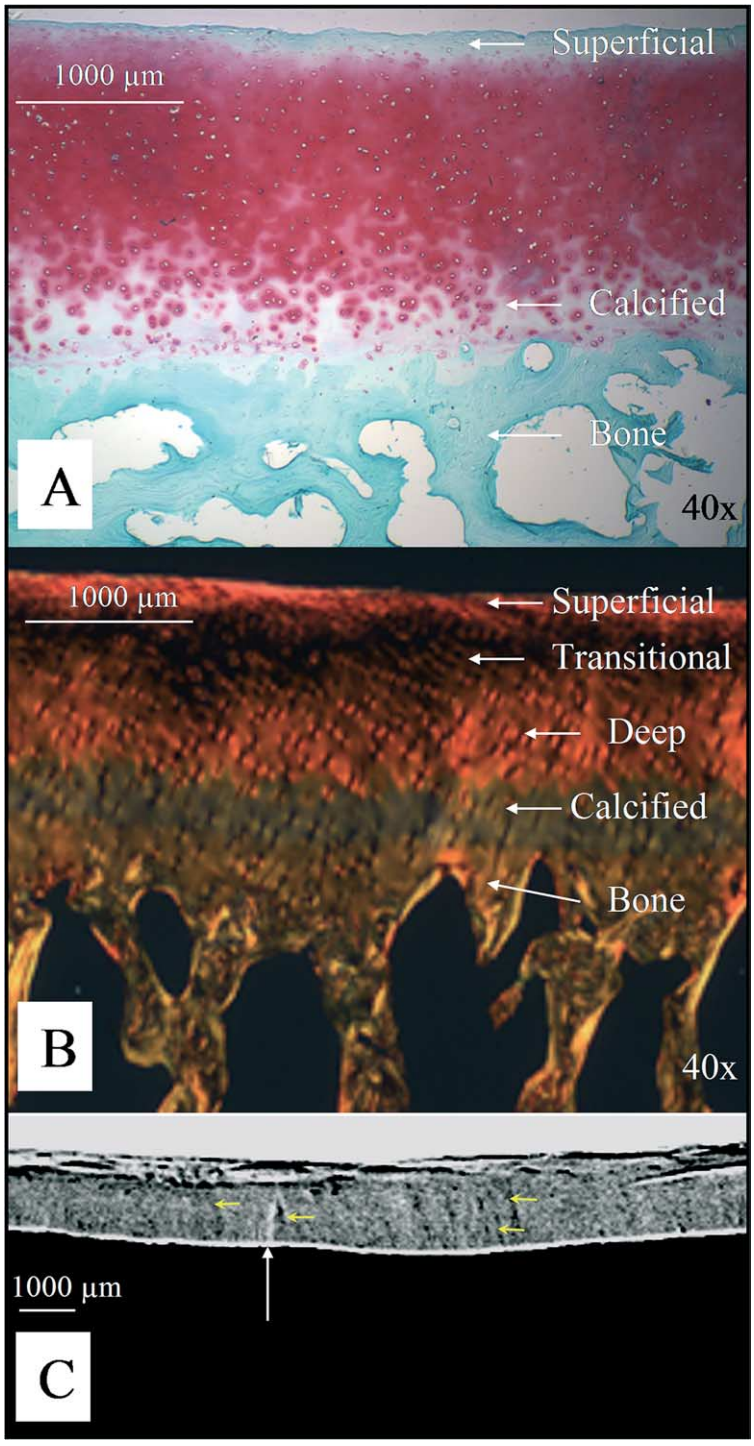

Fig. 1. Safranin O stained section of cartilage and bone from normal-looking cartilaginous surface of a talar dome. B. Polarized light micrograph of a picrosirius red-stained section of cartilage and subchondral bone from a talar dome showing the normal birefringent pattern of the uncalcified zones of the cartilage. C. DEI absorption image of a 5 mm thick specimen from which the section in B was taken. Faint vertical striations are visible throughout the cartilage (yellow arrows). The cartilage/bone interface is identified at the white arrow. This specimen was prepared for imaging by the 'fracture method'.

independent of location. These striations extend from the bottom of the deep zone to the superficial zone, at which point they arc. Some striations begin to arc a bit deeper in the cartilage than others, but all arc within the superficial 25%.

Each of the specimens (both talus and femoral head specimens) had been imaged at least 5 times with similar results – the vertical structural orientation was repeatedly observed, and at each of the rocking curve points tested.

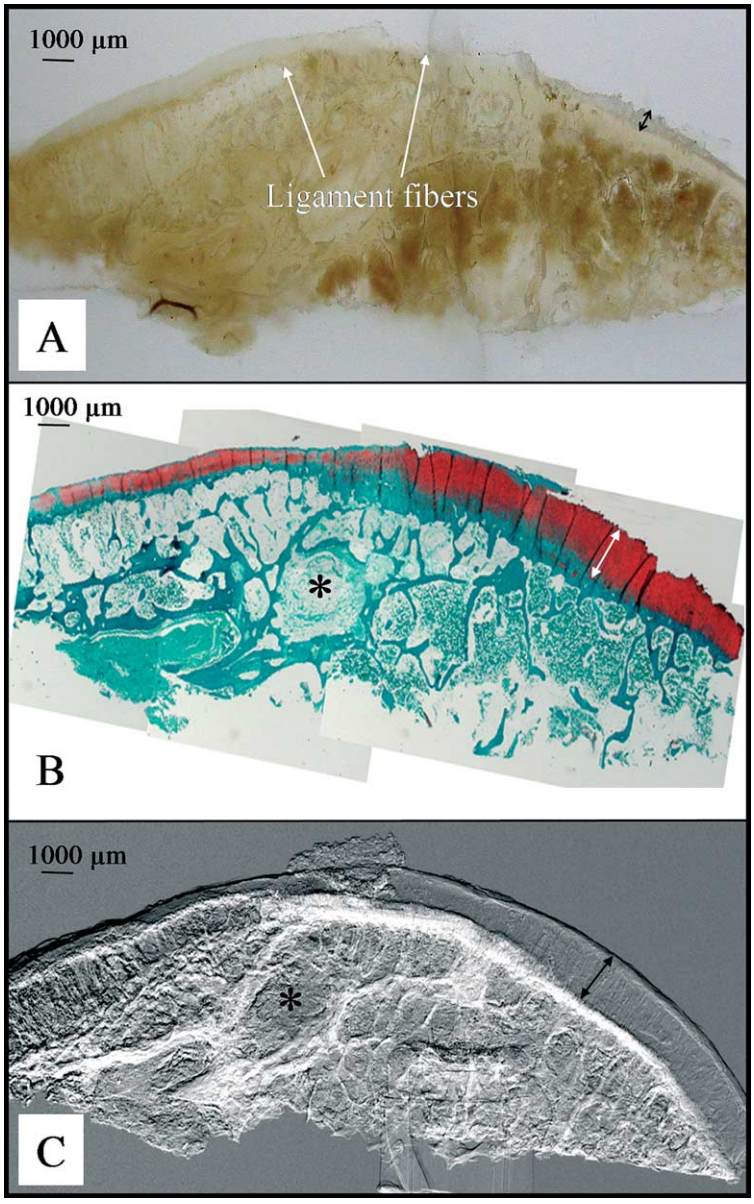

Fig. 2. A photograph of a 1 cm thick piece of normal-looking cartilage (double-headed arrow on the right side of the photograph and subchondral bone from a femoral head removed during surgery for replacement by a prosthetic. Because the specimen was taken from the region around the ligament of the head of the femur, ligamentous fibers obscure the cartilage on the left and central portions of the image. B. Safranin O stained section taken from the specimen in A showing the uncalcified cartilage staining in red (between arrows) and calcified cartilage and bone in green (10×). The damage to the superficial zone cartilage resulted post-imaging. C. Slope of the rocking curve image of the same specimen showing the uncalcified cartilage (double-headed arrow) and calcified cartilage and bone beneath. Vertical striations are visible within the normal-looking cartilage on the right (double-headed arrow), but are obscured by ligamentous fibers on the left and central regions. It is important to note that the DE image here is a composite image of numerous histological sections like those shown in Fig B. A bone cyst can be seen at the *. This specimen was prepared for imaging by the 'fracture method'.

Discussion

Here, we show for the first time, the radiographic detection of a vertical orientation that we believe to be the structural organization of collagen fiber bundles within articular cartilage. Conventional radiography is not capable of allowing visualization of cartilage, and only recently has cartilage been shown to be visible through X-ray imaging[32–34]. The present work extends this capability to cartilage characteristics at a higher level of resolution as capable at the ELETTRA synchrotron in Trieste, Italy. Our previous work has shown that DEI has the potential for detection of cartilage lesions in intact joints[32,33], thus providing incentive toward the development of a non-synchrotron based DEI system (which is in progress) for the clinical detection of early degenerative joint disease. This technology would provide the basis for the testing of agents or activities that may stop or even reverse the disease process.

As DEI is capable of detecting the refraction and scatter rejection properties, in additional to the apparent absorption of a tissue, it could be assumed that the resultant high

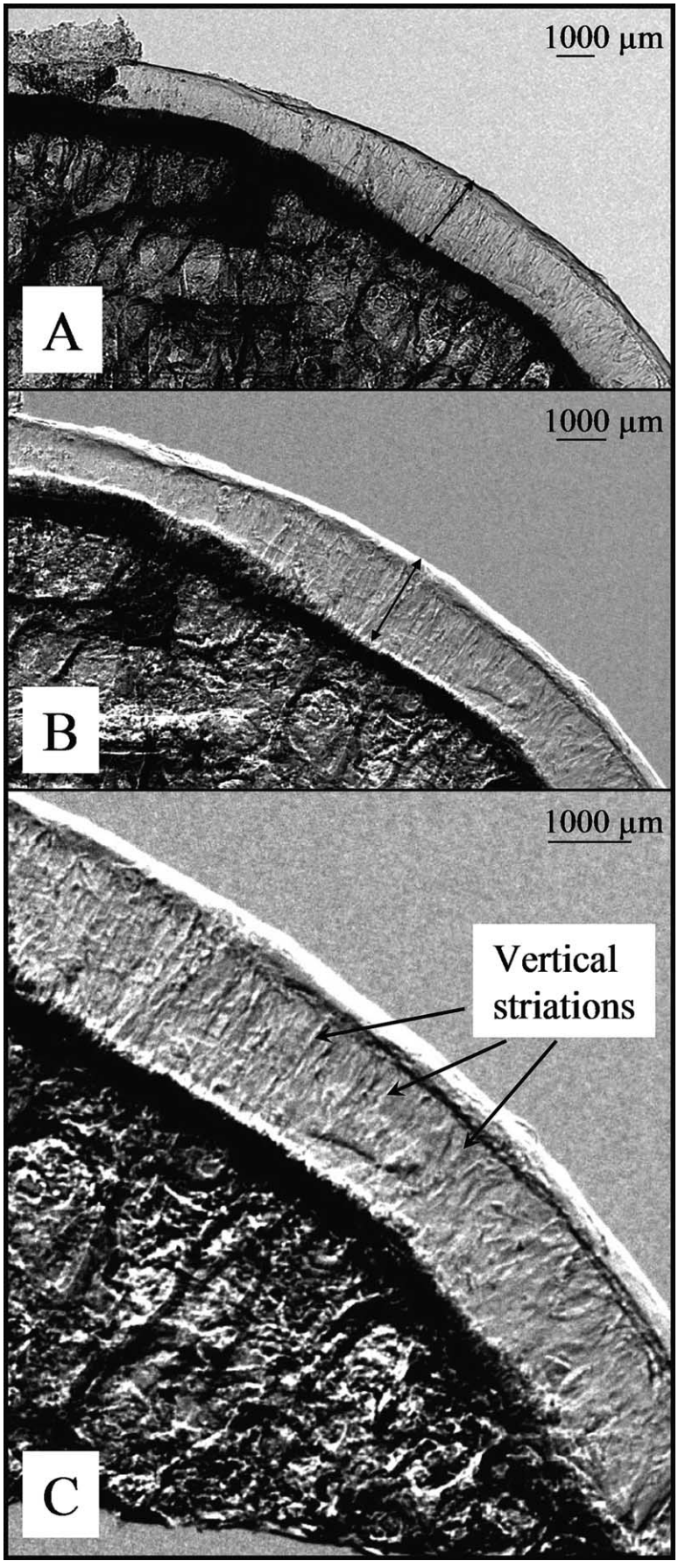
1000 µm
A
1000 µm
B
1000 µm
Vertical striations
C

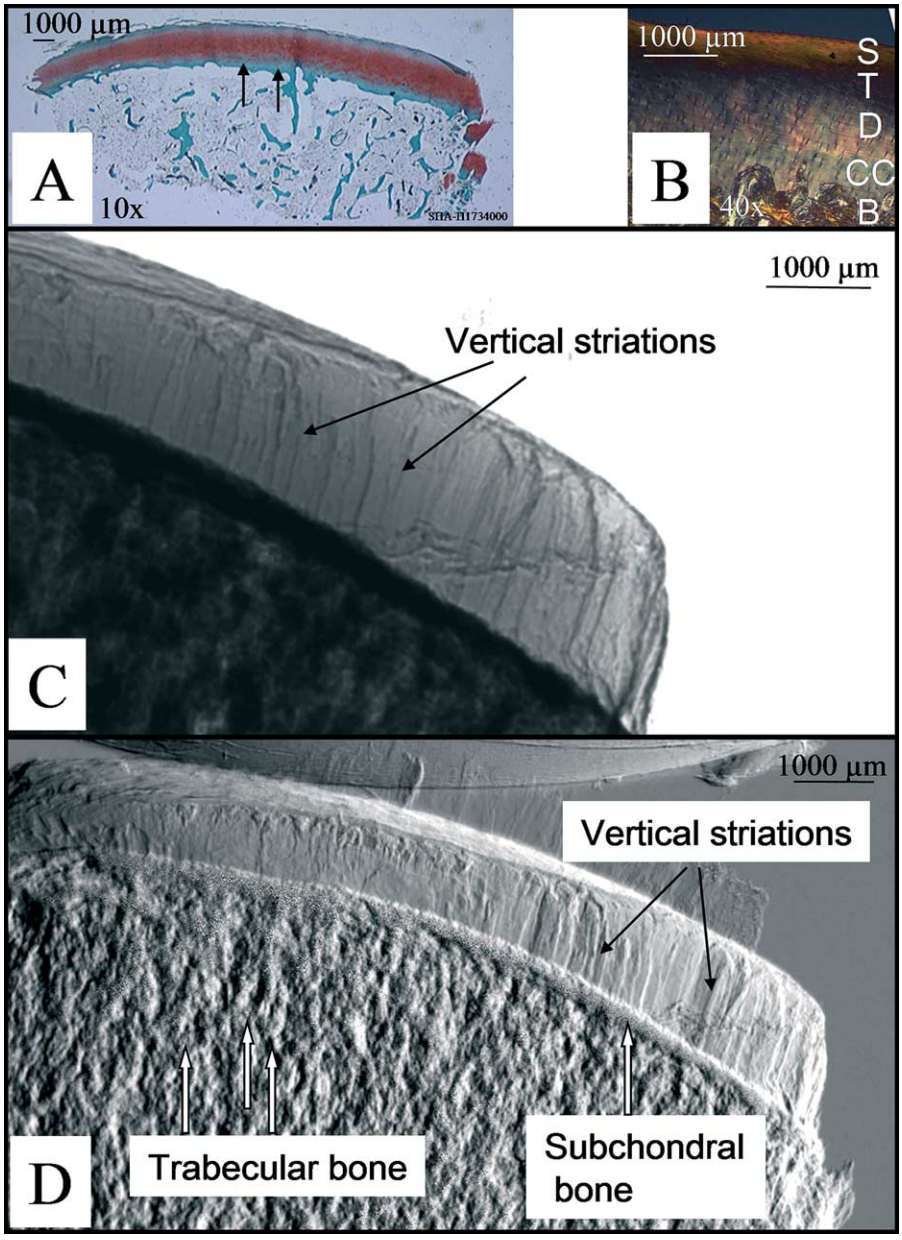

Fig. 4. A Safranin-O stained section of a normal-looking region of the superior pole of the femoral head (10×). The arrows demarcate the bone/cartilage interface. B. A polarized light micrograph of a representative femoral head specimen showing the zones of cartilage (S=superficial, T=transitional, D=deep, CC=calcified cartilage) and subchondral bone (B). C An apparent absorption and, D. a refraction image, taken at 17 KeV, of normal-looking cartilage of a femoral head showing vertical striations, with arcing within the upper cartilage zones. This specimen was prepared for imaging by the 'drill saw method'.

contrast images may show tissue characteristics unavailable through other contrast mechanisms. As demonstrated in the resulting images of this study, the technique is particularly sensitive to the edges of details, where sudden changes in the real part of the refraction index determine strong refraction effects. For this reason, an edge enhancement effect is perceived, even from non-absorbing or weakly absorbing objects. Therefore, details not detectable with conventional techniques are clearly visible. It should be noticed, however, that DEI sensitivity is maximized for edges lying in the direction perpendicular to the diffraction plane (i.e. along the beam width).

The collagen fiber bundles, which are faintly observable at the peak of the rocking curve where there is little refraction information, become quite apparent when the image is taken on the slope of the rocking curve

Fig. 3. An enlarged apparent absorption image and, 3B. refraction image, taken at 25 keV, of the normal-looking region of the same specimen in Fig. 2C showing the vertical striations within the cartilage. 3C is a more enlarged refraction image view of the vertical striations showing greater detail.

where refraction is greatest. We hypothesize that this fiber bundle organization is actually the detection of density jumps between major collagen bundles. Gaps in between bundles are most likely filled with proteoglycan containing more water, thus, generating regions of lower density between the compact collagen fiber structures.

Certainly, striations have been previously observed in cartilage through both SEM, optical coherence tomography (OCT), and MRI. EM studies[6–12] have demonstrated the arcade arrangement of collagen fiber bundles in the articular cartilage of human and rabbit knee joints. Specifically, it has been observed that articular cartilage has defined vertical fibers that can be traced to the cartilage surface, at which point they arc and flatten. However, tracing the full extent of a single collagen fiber or bundle from beginning to end remains elusive.

Collagen orientation has also been detected with OCT imaging whereby the polarization sensitivity of cartilage was presumably related to the structural organization of the collagen fibers[39] and cartilage changes in polarization sensitivity correlated with changes in human cartilage collagen organization in vitro[40].

Waldschmidt *et al.*[14] suggested that the alternating hypointense and hyperintense bands that they observed perpendicular to the subchondral bone through MRI, corresponded to collagenous tissue and chondrocytes with intercellular matrix, respectively.

Although a precise correlation between histological cartilage zones and MRI laminae has yet to be carried out, high resolution MRI work by Xia *et al.*[20] showed that μMRI zones based on T2 characteristics are statistically equivalent to the histological zones in unstained sections. Their results demonstrated that cartilage can be subdivided into three structural zones based on the regional characteristics of T_2 relaxation.

Furthermore, in a study by Foster *et al.*[15], striations were observed in knee joints recovered post-mortem using high resolution MRI. They also suggested that the variations in MRI density were due to the periodic presence of plates of high collagen and proteoglycan content. The work of the present study addresses their request for others to search, by other techniques, for the structural heterogeneity that they have described. We have, thus, shown that the structural periodicity/orientation observed through SEM and high resolution MIR can also be demonstrated through the novel X-ray technique, DEI.

Our data are in line with previous studies on the structural organization of joint cartilage. They confirm the model of a vaulting system of collagen fiber bundles interrupted by proteoglycan aggregates. Since these vaults can be seen irrespective of the horizontal alignment of cartilage (we did not use a preferred orientation of the joint specimens) they appear not to be flat but arranged in rotational geometry. The resolution of DEI is limited by the imaging detectors, currently at about five micrometers, at best. It appears reasonable to speculate that, with the advent of high resolution detectors, even more detailed images from tissue structures can be generated. This may permit a destruction-free X-ray light microscopy of three-dimensional samples, when combined with computed tomography. Concerning the example presented here it allows us to predict that DEI may be capable of imaging very early signs of tissue disorganization at the onset of joint cartilage degenerations typical for early stages of osteoarthritis.

Limitations of the study

We acknowledge that this study has limitations. Firstly, our sample number is limited. With only one talus sample and six femoral head samples, we do not have a full representation of cartilage specimens. This is due solely to the fact that we had only one short opportunity to perform our experiments at the synchrotron site. Secondly, as an initial, purely descriptive study, it lacks statistical analyses with polarizing light microscopy.

Acknowledgements

This study was funded by NIH grant RO1-AR048292-02, RO1-AG17762, and EU grant HPRI-CT-1999-50008. We would also like to thank the families of the donors to the Gift of Hope Organ and Tissue Donor Network of Illinois.

References

1. Schenk RK, Eggli PS, Hunziker EB. Articular cartilage morphology. In: Kuettner K, Schleyerbach R, Hascall VC, Eds. Articular Cartilage Biochemistry. New York: Raven Press 1986;3–22.
2. Mow VC, Setton LA, Guilak F, Ratcliffe A. Mechanical factors in articular cartilage and their role in osteoarthritis. In: Kuettner K, Goldberg. Rosemont V, Osteoarthritic Disorders IL, Eds. American Academy of Orthopaedic Surgeons 1995;147–71.
3. Benninghoff A. Form und bau der gelenkknorpel in ihren beziehungen zur funktion. Anat Entwicklungsgesch 1925;76:43.
4. Lillie RD. Microscopy, in Histopathologic Technic and Practical Histochemistry. 3rd Ed. New York, McGraw-Hill, Inc. 1965; 1–21.
5. Dallek M, Jungbluth KH, Holstein AF. Studies on the arrangement of the collagenous fibers in infant epiphyseal plates using polarized light and the scanning electron microscope. Arch Orthop Trauma Surg 1983;101:239–45.
6. Clark JM. The organization of collagen in cryofractured rabbit articular cartilage: a scanning electron microscopic study. J Orthop Res 1985;3:17–29.
7. Clark JM. The organization of collagen fibrils in the superficial zones of articular cartilage. J Anat 1990; 171:117–30.
8. Clark JM. Variation of collagen fiber alignment in a joint surface; a scanning electron microscope study of the tibial plateau in dog, rabbit and man. J Orthop Res 1991;9:246–57.
9. Hwang WS, Li B, Jin LH, Ngo K, Scharchar NS, Hughes GNF. Collagen fibril structure of normal, aging, and osteoarthritic cartilage. J Pathol 1992; 167:425–33.
10. Chen MH, Broom N. On the ultrastructure of softened cartilage: a possible model for structural transformation. J Anat 1998;192:329–41.
11. Kääb MJ, Ito K, Clark JM, Nötzli HP. Deformation of articular cartilage collagen structure under static and cyclic loading. J Orthop Res 1998;16:743–51.
12. Kääb MJ, Ito K, Rahn B, Clark JM, Nötzli HP. Effect of mechanical load on articular cartilage collagen structure: a scanning electron-microscopic study. Cells Tissues Organs 2000;167:106–20.

13. Mollenhauer J, Aurich M, Muehleman C, Irving T. X-ray diffraction of the molecular structure of cartilage. Connect Tissue Res 2003;44:1–7.
14. Waldschmidt JG, Rilling RJ, Kajdacsy-Balla AA, Boynton MD, Erickson SJ. In vitro and in vivo MR imaging of hyaline cartilage: zonal anatomy, imaging pitfalls and pathological conditions. RadioGraphics 1997;17:1387–402.
15. Foster JE, Maciewicz RA, Taberner J, Dieppe PA, Freemont AJ, Keen MC, *et al.* Structural periodicity in human articular cartilage: comparison between magnetic resonance imaging and histological findings. Osteoarthritis and Cartilage 1999;7:480–5.
16. Disler DG, McCauley TR, Wirth CR, Fuchs MD. Detection of knee hyaline cartilage defects using fat-suppressed three-dimensional spoiled gradient-echo MR imaing: comparison with standard MR imaging and correlation with arthroscopy. Am J Roentgenol 1995;165:377–82.
17. Mlynarik V, Degrassi A, Toffanin R, Vittur F, Cova M, *et al.* Investigation of laminar appearance of articular cartilage by means of magnetic resonance microscopy. Mag Res Imaging 1996;14:435–42.
18. Lehner KB, Rechl HP, Gmeinwieser JK, Heuck AF, Lukas HP, Kohl HP. Structure, function, and degeneration of bovine hyaline cartilage: assessment with MR imaging in vitro. Radiology 1989;179:495–9.
19. Xia Y, Farquhar T, Burton-Wurster N, Lust G. Origin of cartilage laminae in MRI. J Magn Reson Imaging 1997;7:887–94.
20. Xia Y, Moody JB, Burton-Wurster N, Lust G. Quantitative in situ correlation between microscopic MRI and polarized light microscopy studies of articular cartilage. Osteoarthritis Cartilage 2001;9:393–406.
21. Modl JM, Sether LA, Haughton VM, Kneeland JB. Articular cartilage: correlation of histologic zones with signal intensity at MR imaging. Radiology 1991;181: 853–5.
22. Xia Y. Magic-angle effect in magnetic resonance imaging of articular cartilage. Invest Rad 2000;35:602–21.
23. Xia Y, Moody JB, Alhadlaq H. Orientation dependence of T2 relaxation in articular cartilage: A microscopic MRI (micro MRI) study. Magn Reson Med 2002; 48:460–9.
24. Xia Y, Moody JB, Alhadlaq H, Hu J. Imaging the physical and morphological properties of a multi-zone young articular cartilage at microscopic resolution. J Magn Reson Imaging 2003;17:365–74.
25. Rubinstein JD, Kim JK, Moraza-Protzner IM, Stanchev PL, Henkelman RM. Effects of collagen orientation on MR imaging characteristics of bovine articular cartilage. Radiology 1993;188:210–26.
26. Erickson SJ, Waldschmidt JG, Czervionke LF. Hyaline cartilage: truncation artifact as a cause of trilaminar appearance with fat-suppressed three-dimensional spoiled gradient-recalled sequences. Radiology 1996;201:260–4.
27. Frank LR, Brossmann J, Buxton RB, Resnick D. MR imaging truncation artifacts can create a false laminar appearance in cartilage. Amer J Roentgenol 1997; 168:547–54.
28. Rubenstein J, Recht M, Disler DG, Kim J, Henkelman RM. Laminar structures on MR images of articular cartilage. Radiology 1997;204:15.
29. Wacker FK, Bolze X, Felsenberg D, Wolf KJ. Orientation-dependent changes in MR signal intensity of articular cartilage: A manifestation of the 'magic angle effect'. Skelet Radiol 1998;27:306–10.
30. Olivier P, Loeuille D, Watrin A, Walter F, Etienne S, Netter P, *et al.* Structural evaluation of articular cartilage. Arthritis Rheum 2001;44:2285–95.
31. Yoshioka H, Haishi T, Uematsu T, Matsuda Y, Anno I, Echigo J, *et al.* MR microscopy of articular cartilage at 1.5 T: orientation and site dependence and laminar structures. Skeletal Radiol 2002;31:505–10.
32. Mollenhauer JA, Aurich ME, Zhong A, Muehleman C, Cole AA, Hasna M, *et al.* Diffraction enhanced x-ray imaging of articular cartilage. Osteoarthritis and Cartilage 2002;10:163–71.
33. Muehleman C, Chapman LD, Kuettner KE, Mollenhauer J, Rieff J, Zhong Z. Radiography of rabbit articular cartilage with diffraction enhanced imaging. Anatomical Record. Anat Rec 2003;272A: 392–7.
34. Li J, Zhong Z, Lidtke R, Kuettner KE, Peterfy C, Aliyeva E, *et al.* Radiography of Soft Tissue of the Foot and Ankle with Diffraction Enhanced Imaging. Journal of Anatomy. J Anat 2003;202:463–70.
35. Muehleman C, Bareither D, Huch K, Cole A, Kuettner KE. Prevalence of degenerative morphological changes in the joints of the lower extremity. J Osteoarthritis Cart 1997;5(1):1–15.
36. Uebelhart DE, Thonar EJ-MA, Pietryla DW, Williams JM. Elevation in urinary levels of pyridinium crosslinks of collagen following chymopapain-induced degradation of articular cartilage in the rabbit knee provides evidence of metabolic changes in bone. Osteoarth Cart 1993;1:185–92.
37. Chapman D, Thomlinson W, Johnston RE, Washburn D, Pisano E, Gmur N, *et al.* Diffraction enhanced x-ray imaging. Phys Med Biol 1997;A447:556–68.
38. Rosenberg L. Chemical basis of the histological use of Safranin O in the study of articular cartilage. J Bone Joint Surg (AM) 1971;53:69–82.
39. Herrmann JM, Pitris C, Bouma BE, Boppart SA, Jesser CA, Stamper DL, *et al.* High resolution imaging of normal and osteoarthritic cartilage with optical coherence tomography. J Rheumatol 1999;26: 627–35.
40. Drexler W, Stamper D, Christine J, Li X, Pitris C, Saunders K, *et al.* Correlation of collagen organization with polarization sensitive imaging of in vitro cartilage: implication for osteoarthritis. J Rheumatol 2001;28:1311–8.